A Dynamic Loads Scaling Methodology for Helicopter Rotors

Louis Mirandy*
Boeing Vertol Company, Philadelphia, Pa.

A method for scaling vibratory loads between dynamically dissimilar rotors is developed. It is based upon separating the blade response into contributions from each of its natural modes in order to account for dynamic differences between the model and prototype. The procedure is applied to test data obtained from different size rotors. Good correlation results. In addition, the modal approach is shown to provide a practical means of determining vibratory hub loads and blade deflections (which are usually difficult to measure directly) from blade bending moment measurements which are relatively easy to obtain.

Introduction

MODEL testing of helicopter rotors is a useful aid to various aspects of prototype design such as performance, stability, dynamic loads, and the exploration of new concepts. Ormiston[1] gives an excellent survey of helicopter modelling usage and techniques. In this work, we will consider specifically the application of model rotor vibratory loads to prototype dynamic design.

The application of model rotor testing to prototype dynamic design has historically required the construction of a model which is dynamically as well as aerodynamically similar. All model loads can then be scaled by simple geometric factors. While such an approach greatly facilitates the scaling of dynamic loads, it requires the often difficult task of building a dynamically similar model, and furthermore it limits the application of model test results to a specific prototype design. Clearly, great value could be derived from the capability to scale vibratory loads between a nondynamically similar model and prototype. The principal difficulties are that, in general, the scale factors will depend on both the dynamic character of the applied loads and the point on the structure at which the measured loads are being scaled. For example, dynamic scale factors for one per rev loads may differ from those for two per rev loads, while in addition, the ratio of model to full scale bending moments at, say, .20 radius may differ from that at .40 radius for all forcing frequencies. To overcome these difficulties we separate the response of the rotor according to its frequency and modal content. The modal separation enables the response of a complex structure to be conveniently expressed in terms of a minimum number of variables. The technique of scaling these variables is developed herein.

Apart from dynamic similarity, another problem area in model rotor testing is the accurate determination of fixed system vibratory hub loads. The problem exists because in order to be sensitive enough to measure rotor loads, the balance will most likely also be flexible enough to contain resonances in the frequency range of interest. An important spin-off of the modal separation process used for scaling is that it enables the accurate determination of fixed system vibratory hub loads from blade bending moment and root hinge angular deflection measurements. The current emphasis on helicopter vibration makes this capability increasingly important.

Received Feb. 7, 1977; presented as Paper 77-424 at the AIAA/ASME 18th Structures, Structural Dynamics, and Materials Conference, San Diego, Calif., March 21-23, 1977; revision received July 18, 1977.

Index categories: Propeller and Rotor Systems; Helicopters; Structural Dynamics.

*Currently Project Engineer, General Electric Co., Space Division, Valley Forge, Pa.

Overview

Figure 1 summarizes the major steps of the scaling procedure. We begin with a model and prototype having the same nondimensional aerodynamic parameters. These include geometric properties such as blade twist, planform taper, airfoil type, etc.; and operating conditions such as advance ratio, inflow ratio, and blade pitch setting. The model may be scaled to have either the same Mach number or Reynold's number as the prototype, whichever is deemed more important. (The models reported on later in this study were all roughly Mach scaled.) The key point to keep in mind is that the model and prototype should experience, as nearly as possible, the same nondimensional aerodynamic loading. And in many cases of practical importance, differences in Mach number or Reynold's number will produce a negligible effect. It is important to point out that for hingeless rotors, cyclic pitch and not hub moment should be matched on the model and prototype in order to obtain aerodynamic similarity. On the other hand, in most practical applications on both hingeless and articulated rotors, thrust coefficient is a better parameter to match than collective pitch.

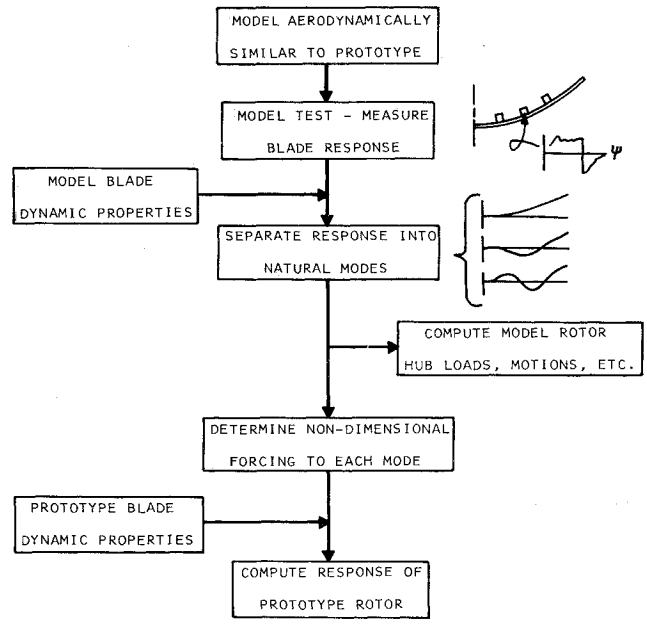

Fig. 1 Steps in scaling procedure.

During the model test some form of blade dynamic response, usually bending moment at several radial stations, is measured. In general, this response is comprised of the aggregate of separate responses from each of the blade natural modes. The individual contributions of the dominant modes are next computed with the aid of known model dynamic properties. At this point the modal contributions may be used to calculate other model response parameters such as fixed system hub loads. More important, we are now able to compute the nondimensional airloads which caused the response in each mode. These airloads in turn are used to compute the dynamic response of the prototype design. In fact, these same airloads may be used to compute the dynamic response of any rotor which is aerodynamically similar to the model.

Scope

The methodology is developed and demonstrated for steady-state operating conditions in which blade dynamic loads are repeated rotor cycle after rotor cycle. The dynamic response is then conveniently expressed in terms of its harmonic content, rather than as a time history. It should be remarked, however, that the methodology is not dependent on the harmonic character of the loads so that the scaling procedure is easily modified to handle general time histories, thus enabling the method to be used for maneuver conditions. This is discussed in more detail later.

We exclude from this work rotor instabilities and conditions at which significant amounts of blade stall exist. In such circumstances the key element is often the airloads that result from the blade motions themselves. For dynamically dissimilar rotors the blade motions will differ and hence the onset of stall or instability will occur at different operating conditions. The scaling method presented herein accounts only for simple linear airloads due to blade motions, and as such cannot adequately handle instabilities or blade stall.

The methodology will be developed in detail for blade uncoupled flapwise response. (The blade flapwise, chordwise and torsional directions are illustrated in Fig. 2.) The scaling of blade torsional loads is analogous to the flap case, for conditions in which nonlinearities due to stall or compressibility are not in evidence. The additional considerations necessary for scaling chordwise loads are pointed out in the next section. The method can be further extended to incorporate coupled flap-chord-pitch blade modes. Finally, the modal scaling approach, presented in this work, can most likely be used in other, analogous, (nonhelicopter) model testing applications.

Analytical Development

The dynamic response of a rotor blade may be expressed as the sum of the individual responses occurring in each of the blade's natural modes. For example, the flapwise deflection w at a given radial position r may be written

$$w(r,t) = \sum_{i=1}^{\infty} Z_i(r)\, q_i(t) \tag{1}$$

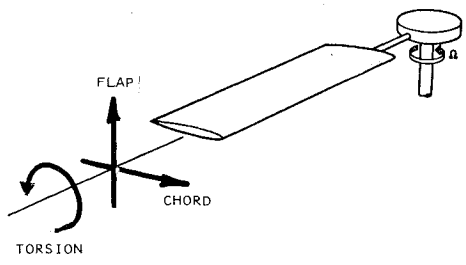

Fig. 2 Blade motions.

where Z_i is the deflection shape of the ith mode and q_i is the generalized coordinate, a measure of the participation of the ith mode. Since Z_i is simply the shape assumed by the blade when vibrating in the ith natural mode, it may be normalized to any convenient value. Standard practice in the helicopter industry has been to assign the modal tip deflections a value of unity, i.e., $Z_i(R) = 1$. Then q_i is the blade tip motion due to participation of the ith mode. Corresponding to each modal deflection shape (Z_i) are unique radial distributions of bending moment (M_{yi}), shear (V_{Zi}), and slope (dZ_i/dr). These quantities (Z_i, M_{yi}, etc.) depend only on the blade physical properties and rotational speed, while the generalized coordinates reflect the applied forcing and blade dynamic characteristics.

It is important to recognize that all possible states of flapwise deflection can be described by Eq. (1). Completely analogous expressions exist for slope, bending moment, and shear. Thus, if any one of these four quantities are known, the remaining three may be uniquely determined. The generalized coordinate representation provides a convenient means of going from motions to moments to shears. Finally, it will be noted that, in general, it requires an infinite number of modes to completely define the response. Of course, in most practical applications only a few modes are required, because the response in higher modes becomes negligible. For example, we have found that three elastic flap modes are usually ample. With this brief introduction to the modal representation of blade response, we proceed to the determination of generalized coordinates from test measurements.

Separation of Response into Normal Modes

First some form of the model blade response is recorded during the test. Let us assume that we have flapwise bending moment measurements at a number of different radii. The moment at any particular radial station, $r = r_j$, may be expressed as

$$m_y(r_j,t) = \sum_i M_{yi}(r_j)\, q_i(t) \tag{2}$$

where the "modal moments" M_{yi} are readily determined from theory (they are outputs in most blade natural frequency computer analyses), or they may be measured directly in a shake test. They represent the bending moment distribution per unit motion in their respective modes. If bending moments are measured at m discrete radial stations, we may use these data to solve for a finite number of generalized coordinates. The appropriate equations are

$$\begin{bmatrix} M_{y1}(r_1) & M_{y2}(r_1) & \cdots & M_{yn}(r_1) \\ \cdot & \cdot & \cdot & \\ \cdot & \cdot & \cdot & \\ \cdot & \cdot & \cdot & \\ \cdot & \cdot & \cdot & \\ M_{y1}(r_m) & \cdots & & M_{yn}(r_m) \end{bmatrix} \begin{Bmatrix} q_1 \\ q_2 \\ \cdot \\ \cdot \\ \cdot \\ q_n v \end{Bmatrix} = \begin{Bmatrix} m_y(r_1,t) \\ m_y(r_2,t) \\ \cdot \\ \cdot \\ \cdot \\ m_y(r_m,t) \end{Bmatrix} \tag{3}$$

Thus there are m linear algebraic equations for the n unknown q_i. A unique solution exists for $n=m$, and for $n<m$ a least-squares solution may be sought. In this last case the error in the solution of the ith equation is given by

$$\epsilon_i = m_y(r_i) - \sum_{j=1}^{n} M_{yj}(r_i)\, q_j \tag{4}$$

The equations will be satisfied in the least-squares sense when

$$\sum_{i=1}^{m} \epsilon_i^2$$

is a minimum. It is easily shown that this condition results in the following set of n equations:

$$[M_y]^T [M_y] \{q\} = [M_y]^T \{m\} \tag{5}$$

where $[M_y]$ is the matrix of modal moments on the left-hand side of Eq. (3) and $[M_y]^T$ is its transpose.

To provide an ability to assess the goodness of fit, it is recommended that the blades be instrumented with more gages than the number of modes to be analyzed, and the least squares solution used. The process is analogous to drawing a smooth curve through a number of data points rather than trying to draw the curve through each and every point.

The equations for the generalized coordinates may either be solved at a sufficient number of discrete values of time or the $m_y(r,t)$ may be replaced by their harmonic components in the case of steady-state operating conditions. The form of the raw data and ultimate use of the generalized coordinates will dictate the more expeditious route.

An articulated rotor has rigid-body flapping freedom which does not produce any bending moment. To determine the amount of rigid-body motion we must measure blade root flap angle (or a flapwise acceleration on the blade). The flap angle contains elastic as well as rigid-body motion so that

$$\beta(t) = \beta_M(t) - \sum_i \frac{\mathrm{d}Z_i(0)}{\mathrm{d}r}\, q_i \tag{6}$$

where β is the flap angle due to rigid-body motion and β_M is the measured flap angle. The q_i are known after solving Eq. (5).

Scaling of Generalized Coordinates

The generalized coordinates serve as excellent quantities to scale between model and prototype since they can be used to compute the loads and motions at any point on the blade. The equation for the ith flapwise coordinate, q_i, may be written

$$q_i'' + (\omega/\Omega)_i^2 q_i = \frac{\rho c R^3}{N_i} \int_1^0 p_\beta Z_i \mathrm{d}x \tag{7}$$

where

N_i = generalized mass in the ith mode $= \int Z_i^2 \mathrm{d}m$
$(\omega/\Omega)_i$ = natural frequency of the ith mode in per rev
ρ = air density
c = blade chord
R = blade radius
$(\ )'$ = $\mathrm{d}(\ )/\mathrm{d}\psi$, $\psi = \Omega t$

In general the nondimensional flap forcing distribution p_β will depend upon the blade motion and hence upon the q_j themselves. Let us separate p_β into a part that depends upon blade motion, $p_m(q_j)$, and a part that is independent of blade motion, p_0. Then Eq. (7) may be rewritten as

$$N_i/\rho c R^3 \{q_i'' + (\omega/\Omega)_i^2 q_i\} - \int p_m(q_j) Z_i \mathrm{d}x = F_i \tag{8a}$$

$$F_i \equiv \int p_0 Z_i \mathrm{d}x \tag{8b}$$

The generalized coordinates are known from the model test and if the functional form of p_m is known, then we may solve Eq. (8) for F_i. The nondimensional forces F_i, so found, apply to any aerodynamically similar rotor, provided its mode shapes Z_i do not differ appreciably from those of the model. Equation (8) can then be used to solve for the prototype generalized coordinates, since its physical properties (N_i, $(\omega/\Omega)_i$, c, etc.) are presumably known along with the forcing F_i. The accuracy of the procedure depends upon how good the representation for p_m is and how well the mode shapes of the model and prototype agree. In most practical applications differences in mode shape are not a major factor. Nevertheless, a procedure which accounts for such differences is presented in Appendix A. The aerodynamic loading due to blade motions has been determined on the basis of quasisteady linear aerodynamics in Appendix B. The results are

$$-\int p_m Z_i \mathrm{d}x = \sum_j \{(c_{ij} + \mu d_{ij}\sin\psi) q_j' + (\mu s_{ij}\cos\psi + \mu^2 r_{ij}\sin 2\psi) q_j\} \tag{8c}$$

where the coefficients (c_{ij}, d_{ij}, etc.) are defined in Appendix B. Eqs. (8a), (8b), and (8c) are sufficient to scale the generalized coordinates determined from model testing to corresponding prototype values. The procedure may be vastly simplified if we neglect intermodal coupling and time-dependent coefficients in Eq. (8c). Then

$$-\int p_m Z_i \mathrm{d}x \approx 2N_i (\omega/\Omega)_i \zeta_i q_i'/\rho c R^3 \tag{9a}$$

where ζ_i is the uncoupled critical damping ratio in the ith mode. It is given by

$$\zeta_i = \frac{\rho a c R^2}{4N_i (\omega/\Omega)_i} \int_{xc}^{1} x Z_i^2 \mathrm{d}x \tag{9b}$$

With these simplifications Eq. (8) may be rewritten

$$N_i/\rho c R^3 \{q_i'' + 2(\omega/\Omega)_i \zeta_i q_i' + (\omega/\Omega)_i^2 q_i\} = F_i + e_i \tag{10}$$

where e_i is the error introduced by neglecting all terms due to blade motion except for diagonal time-independent damping. A theoretical solution of the equations of motion would feel the effect of both errors in the representation of F_i and in neglected terms e_i, whereas the scaling procedure is sensitive only to the difference in e_i between the model and prototype. If the nondimensional error e_i were the same for model and prototype there would be no scaling error!

We will now concentrate on the equations for steady-state harmonic response. It will be assumed that the harmonic components of the model's generalized coordinates have already been determined from blade bending moment and flap angle data. The following notation will be adopted:

$$q_i = \sum_k q_{ikc}\cos k\psi + q_{iks}\sin k\psi \tag{11a}$$

$$F_i = \sum_k a_{ik}\cos k\psi + b_{ik}\sin k\psi \tag{11b}$$

Upon substituting the above into Eq. (10) with $e_i = 0$, we obtain

$$\begin{Bmatrix} a_{ik} \\ b_{ik} \end{Bmatrix} = [T_k] \begin{Bmatrix} q_{ikc} \\ q_{iks} \end{Bmatrix} \tag{12a}$$

$$[T_K] = N_i/\rho c R^3 \begin{bmatrix} (\omega/\Omega)_i^2 - k^2 & 2(\omega/\Omega)_i \zeta_i k \\ -2(\omega/\Omega)_i \zeta_i k & (\omega/\Omega)_i^2 - k^2 \end{bmatrix} \tag{12b}$$

Equations (12) may be used to solve for the force coefficients a_{ik} and b_{ik} using the model values of q_{ikc} and q_{iks}. Equations (12) may then be inverted to determine the prototype q_{ikc} and q_{iks} using the now known values of a_{ik} and b_{ik}. Thus,

$$\begin{Bmatrix} q_{ikc} \\ q_{iks} \end{Bmatrix}_P = [T_K]_P^{-1}[T_K]_M \begin{Bmatrix} q_{ikc} \\ q_{iks} \end{Bmatrix}_M \tag{13}$$

where the subscripts P and M have been used to denote prototype and model, respectively.

When the harmonic coefficients in Eqs. (11a) and (11b) are substituted into Eqs. (8a) and (8c) a more precise, albeit cumbersome, set of scaling equations evolve. The resulting set of linear algebraic equations, having both intermodal and interharmonic couplings, are given in Appendix C.

Maneuver Conditions

Maneuver conditions can be analyzed if we treat the response as an arbitrary time history. First the model's generalized coordinates are computed from bending moment data at a sufficient number of discrete times to adequately define the time variation. Next Eq. (8a), in conjunction with either (8c) or (9), must be used to calculate the $F_i(t)$. This evaluation will require numerical differentiation of the already determined model q_i. With $F_i(t)$, the prototype response may be found by integrating the same system of differential equations (8a) using prototype rather than model properties.

Chordwise Scaling

The scaling of blade chordwise response is complicated by the fact that the forcing is largely dependent on flap motions. (The converse is not true.) Thus we must know the flap response before we can proceed to scale chordwise loads. A possible scaling procedure will be briefly outlined.

The equation for the ith chordwise generalized coordinate, v_i, has the form

$$(N_{ci}/\rho cR^3)\{v_i'' + (\omega_c/\Omega)_i^2 v_i\} = F_{ci}(t) + f_{\beta i}(q_j) + f_{ci}(v_j) \tag{14}$$

where

N_{ci} = generalized mass of ith chordwise mode
$(\omega_c/\Omega)_i$ = natural frequency of ith chordwise mode
F_{ci} = nondimensional forcing that does not depend upon blade motions
$f_{\beta i}$ = nondimensional forcing due to flapwise motions, this is comprised of both Coriolus acceleration and aerodynamic terms
f_{ci} = nondimensional forcing due to chordwise motion

In order to use Eq. (14) the functions $f_{\beta i}$ and f_{ci} must be explicitly defined, just as $\int p_m Z_i \, dx$ was defined for the uncoupled flap case. The model data can be used to determine: 1) q_i and v_i from blade flapwise and chording bending data, and 2) F_{ci} from Eq. (14).

The following steps can then be taken to determine the prototype response: 1) scale the flapwise response as explained earlier; 2) use the scaled q_i to compute $f_{\beta i}$ for the prototype; and 3) solve Eq. (14) for v_i.

Rotor Dynamic Loads

As mentioned earlier, it is a relatively easy matter to go from the generalized coordinates to other rotor response parameters such as blade motions, bending moments and shears. Because of their importance, formulas for blade root dynamic loads are summarized in Appendix D.

Extensions for Future Consideration

It is possible to rederive the scaling equations for fully coupled flap-chord-pitch modes. This would be particularly useful for highly twisted and/or soft torsional blades. Other areas which merit future consideration include the treatment of unsteady aerodynamics and the coupling of rotor and hub motions. This last application would enable the analysis of various rotor isolation schemes.

Application to Test Data

The technology developed in the previous section has been applied to model and full-scale helicopter test data. In Fig. 3, scaled midspan flapwise bending moments from 12-ft-diam and 16-ft-diam geometrically similar model rotors are compared to CH-47C forward rotor flight data. The geometric scaling is based upon the load ratios which would exist if the rotors were dynamically similar. It is evident that dynamic scaling is required to collapse the data. The harmonic content of model and full-scale flap bending moments is compared in Fig. 4. Again, it is apparent that the dynamic scaling procedure is necessary to bring the data together. In this case the model was a 1/11-scale tandem rotor helicopter. The test conditions associated with Fig. 4 are for a helicopter in "transition" flight. Here large dynamic rotor loads are caused by the intersection of the blades with their trailing tip vortices. It is an extremely difficult flight regime to analytically predict dynamic rotor loads for single-rotor as well as tandem-rotor helicopters. Thus, the application of a loads scaling methodology is particularly attractive here. A final example is contained in Fig. 5 where model blade torsional loads have been scaled and compared to flight test pitch-link loads.

The referenced work[2] documents a rotor wind tunnel test in which individual blade root shears have been measured along with blade bending moments and root angular motions. This information has been used to produce the time histories shown in Fig. 6. There is good agreement between measured root vertical shears and those synthesized from blade bending moment and flap angle data using the modal approach. The measured root shears were obtained from a hub flexure specially designed for this test (such measurements are unavailable in most rotor tests), whereas blade bending and flap angle data are usually available. In Fig. 7 vibratory hub loads measured on a fixed system balance are compared with those computed from blade data by the modal technique. On the whole, the correlation is good.

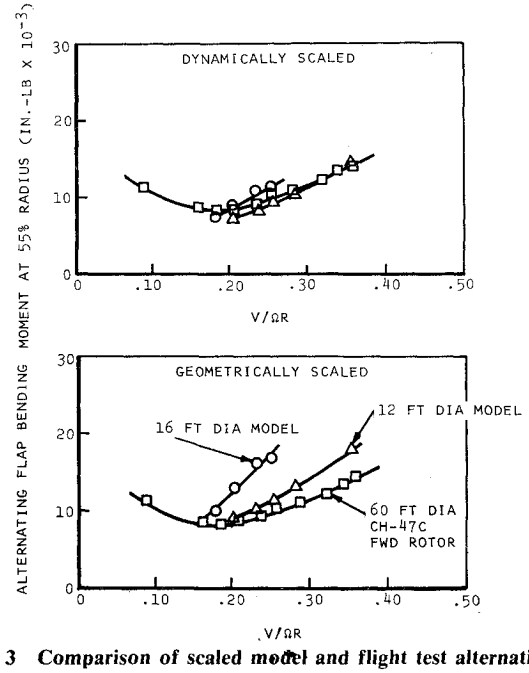

Fig. 3 Comparison of scaled model and flight test alternating flap bending moments. Data from Boeing Vertol wind tunnel and flight tests.

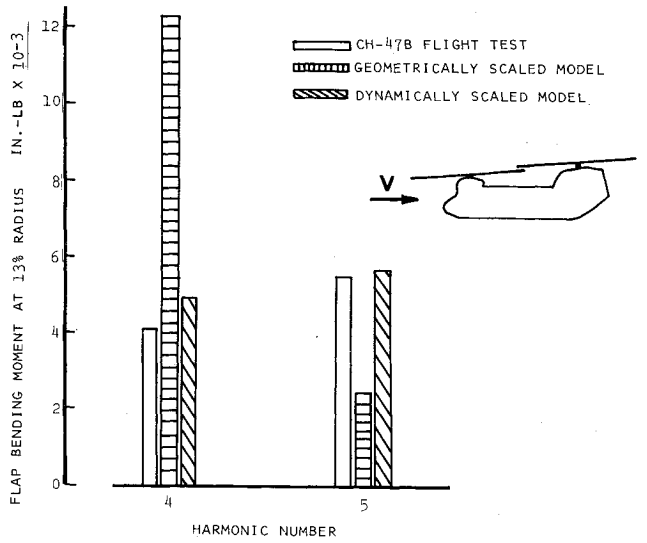

Fig. 4 Comparison of 1/11-scale tandem-rotor helicopter model and flight test flap bending moment harmonic content. Shown for aft rotor, $V/\Omega R = .10$, gross weight = 34,000 lb. Data from Boeing Vertol tests.

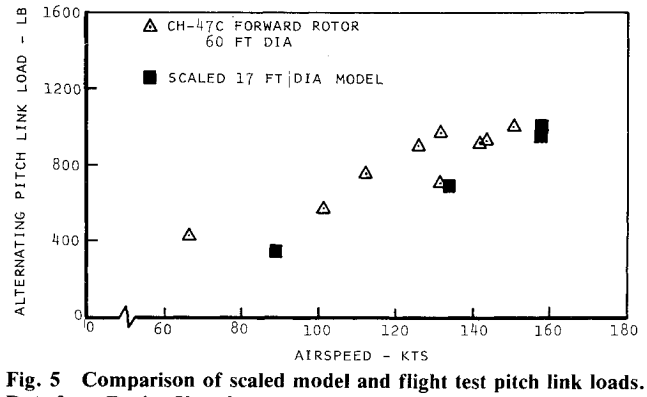

Fig. 5 Comparison of scaled model and flight test pitch link loads. Data from Boeing Vertol tests.

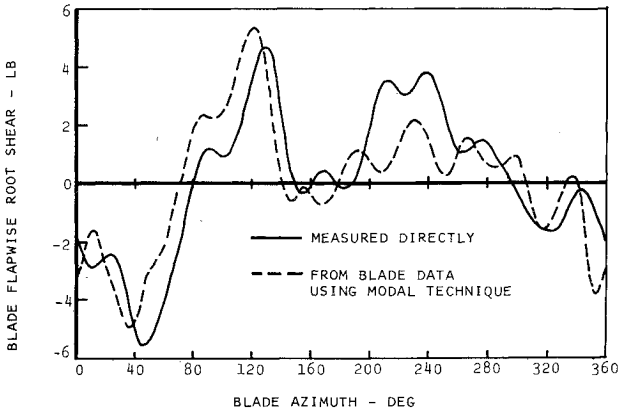

Fig. 6 Comparison of measured and synthesized blade root shears. Shown for $V/\Omega R = .28$, $C_T/\sigma = .062$, $R = 300$ ft/s, 9-ft-diam, 4-bladed model. Data from USAAVLABS technical rept. 66-77.

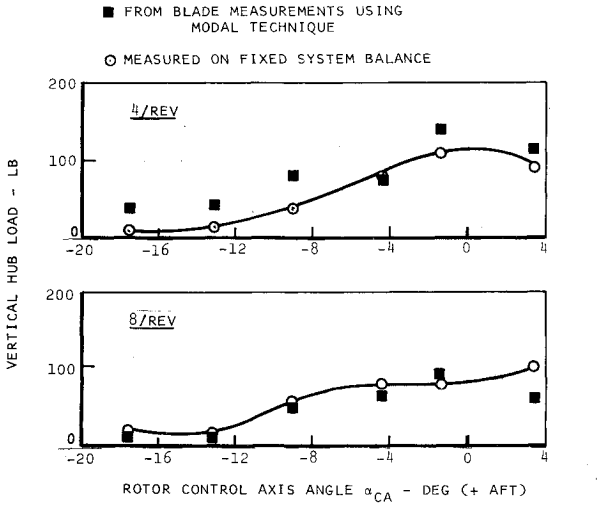

Fig. 7 Comparison of measured and synthesized hub loads. Shown for $V/\Omega R = .30$, $C_T/\sigma = .06$, $V_T = 710$, 17-ft-diam, 4-bladed model rotor. Boeing Vertol wind tunnel data.

An added dividend of the modal approach is that the blade root shears so determined contain all harmonics and thus can be used to approximate fixed system vibratory loads for rotors having any number of blades, rather than just for the rotor tested. This, of course, would not be possible using a conventional fixed system balance, because the balance only feels dynamic loads at n per rev (n = number of blades).

Summary and Conclusions

A methodology for scaling helicopter rotor dynamic loads has been developed and demonstrated using model and full-scale test data. The principal advantages of this capability are:

1) It relieves us from the sometimes difficult task of building a dynamically similar model. For example, blade skin thickness cannot be manufactured to scale on a small model and some sort of compensation is necessary to maintain strict dynamic similarity.

2) Data from one model can be used to assess various prototype designs having different dynamic properties.

A residual benefit of the modal approach, apart from loads scaling, is that fixed system vibratory hub loads can be accurately determined from blade bending moment measurements. The procedure has been illustrated in the text.

In this study, attention has been focused on uncoupled blade flapwise response under steady-state trim conditions. It has been indicated how the method may be extended to handle maneuver loads. The scaling of blade chordwise and torsional freedoms has also been discussed. These topics require additional analytical attention.

Although this method has been developed specifically for helicopter rotors, the modal scaling approach can be profitably used in dynamic modelling situations in which the applied loading between the model and prototype is similar while the structural dynamics are not.

Appendix A: Corrections for Mode Shape

A method to correct for mode shape differences between the model and prototype will be presented. Let Z_{Mi} and Z_{Pi} denote the mode shapes of the model and prototype, respectively. From the model test we may determine

$$F_{Mi} = \int_{xc}^{1} p_0 Z_{Mi} dx \tag{A1}$$

In order to compute the prototype response we need

$$F_{Pi} = \int_{xc}^{1} p_0 Z_{Pi} dx \tag{A2}$$

The Z_{Pi} may be expressed as a series of the Z_{Mi}, since the Z_{Mi} are a complete set in the interval $0 < x < 1$.

$$Z_{Pi}(x) = \sum_j A_{ij} Z_{Mj}(x) \tag{A3}$$

To find the coefficients A_{ij}, we multiply Eq. (A3) by $Z_{Mk}(x)$ and integrate from $x=0$ to $x=1$. This yields the following set of algebraic equations for the A_{ij}:

$$\int_0^1 Z_{Pi}Z_{Mk}\mathrm{d}x=\sum_j A_{ij}\int_0^1 Z_{Mj}Z_{Mk}\mathrm{d}x \tag{A4}$$

The solution is given by

$$[A]=[g][h]^{-1} \tag{A5a}$$

$$g_{ik}=\int Z_{Pi}Z_{Mk}\mathrm{d}x \tag{A5b}$$

$$h_{jk}=\int Z_{Mj}Z_{Mk}\mathrm{d}x \tag{A5c}$$

and

$$F_{Pi}=\sum_j A_{ij}F_{Mj} \tag{A6}$$

Appendix B: Blade Flapwise Equations of Motion

Assumptions: 1) uncoupled flapwise motion; 2) deflections are small and non-linear terms in the generalized coordinates are negligible; 3) aerodynamic forcing is a linear function of angle of attack; 4) quasisteady aerodynamic strip theory; 5) constant rotational speed. Other simplifications will be introduced during the analysis. Expressing the total flapwise motion of the blade as

$$w(x,\psi)=\sum_i Z_i(x)q_i(\psi) \tag{B1}$$

The governing equation for the ith generalized coordinate q_i becomes

$$q_i''+\left(\frac{\omega}{\Omega}\right)_i^2 q_i=\frac{\rho cR^3}{2N_i}\int_{xc}^1 u(C_L u_T+C_D u_P)Z_i\mathrm{d}x \tag{B2a}$$

$$u_T=x+\mu\sin\psi \tag{B2b}$$

$$u_P=\mu\tan\alpha_s-v_{\mathrm{ind}}/\Omega R-\mu\cos\psi\sum_j\frac{\mathrm{d}Z_j}{\mathrm{d}x}\frac{q_j}{R}-\sum_j\frac{Z_j q_j'}{R} \tag{B2c}$$

$$u=(u_T{}^2+u_P{}^2)^{1/2} \tag{B2d}$$

$$\mu=V\cos\alpha_s/\Omega R \tag{B2e}$$

$$\alpha(x,\psi)=\theta(x,\psi)+\arctan(u_P/u_T) \tag{B2f}$$

Rotor geometry and relative velocities are depicted in Fig. 8. C_L and C_D are blade section lift and drag coefficients and x_c is the blade cutout ratio. To determine the part of the forcing dependent on the q_i, the following approximations are made:

$$C_L=a\alpha \qquad C_D=C_{DO} \qquad u=u_T$$

$$\tan^{-1}u_P/u_T=u_P/u_T$$

Then,

$$q_i''+\sum_j[c_{ij}+\mu d_{ij}\sin\psi]q_j'$$

$$+\sum_j[\mu s_{ij}\cos\psi+\mu^2 r_{ij}\sin 2\psi]q_j+(\omega_i/\Omega)^2 q_i$$

$$=(\rho cR^3/N_i)F_i \tag{B3a}$$

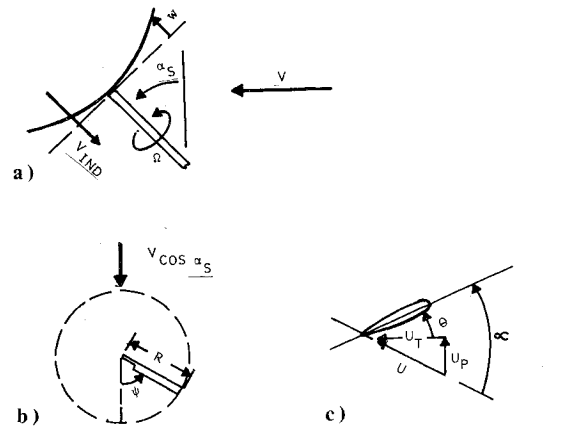

Fig. 8 Rotor operating conditions: a) rotor relative to freestream; b) blade azimuth definition; and c) airfoil angle of attack.

where

$$c_{ij}=\frac{\rho cR^2}{2N_i}(C_{D0}+a)\int_{xc}^1 xZ_iZ_j\mathrm{d}x \tag{B3b}$$

$$d_{ij}=\frac{\rho cR^2}{2N_i}(C_{D0}+a)\int_{xc}^1 Z_iZ_j\mathrm{d}x \tag{B3c}$$

$$s_{ij}=\frac{\rho cR^2}{2N_i}(C_{D0}+a)\int_{xc}^1 xZ_i(\mathrm{d}Z_j/\mathrm{d}x)\mathrm{d}x \tag{B3d}$$

$$r_{ij}=\frac{\rho cR^2}{2N_i}(C_{D0}+a)\int_{xc}^1 Z_i(\mathrm{d}Z_j/\mathrm{d}x)\mathrm{d}x \tag{B3e}$$

$$F_i=\text{the part of }\int_{xc}^1 u(C_L u_T+C_D u_P)Z_i\mathrm{d}x \tag{B3f}$$

that does not depend on the blade motion.

Appendix C: Flapwise Harmonic Response

For steady-state trim conditions, F_i and q_i may be expressed as

$$q_i=q_{i0}+\sum_k(q_{ikc}\cos k\psi+q_{iks}\sin k\psi) \tag{C1}$$

$$F_i=a_{i0}+\sum_k(a_{ik}\cos k\psi+b_{ik}\sin k\psi) \tag{C2}$$

If we substitute the above into the equations of motion (B3) and equate like harmonic powers, we obtain

$$\begin{array}{l}\text{Mode 1}\\ \text{Mode 2}\\ \\ \\ \text{Mode } m\end{array}\left[\begin{array}{c|c|c|c}[M]_{11} & [M]_{12} & \cdots & [M]_{1m}\\ \hline [M]_{21} & [M]_{22} & & [M]_{2m}\\ \hline \vdots & \vdots & & \vdots\\ \hline [M]_{m1} & [M]_{m2} & \cdots & [M]_{mm}\end{array}\right]\left[\begin{array}{c}\{q_{1k}\}\\ \{q_{2k}\}\\ \vdots\\ \{q_{mk}\}\end{array}\right]=\left[\begin{array}{c}\{F_{1k}\}\\ \{F_{2k}\}\\ \vdots\\ \{F_{mk}\}\end{array}\right] \tag{C3a}$$

where off-diagonal submatrices are intermodal coupling terms and where

$$\lfloor q_{ik}\rfloor=\lfloor q_{i0}q_{i1c}q_{i1s}q_{i2c}q_{i2s}\cdots\cdots\rfloor \tag{C3b}$$

$$\lfloor F_{ik}\rfloor=\lfloor a_{i0}a_{i1}b_{i1}a_{i2}b_{i2}\cdots\cdots\rfloor \tag{C3c}$$

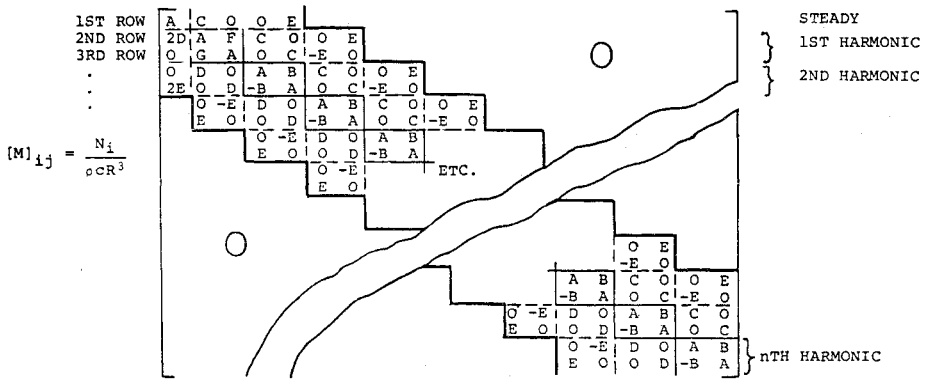

(C3d)

The quantities A, B, C, D, E, F, G are dependent on the harmonic number k: for odd-numbered rows, $k=$ (row no. -1)/2; for even-numbered rows, $k=$(row no.)/2; and,

$$A=\begin{cases}(\omega_i/\Omega)^2-k^2 & (i=j)\\ 0 & (i\neq j)\end{cases}$$

$$B=kc_{ij}$$

$$C=\mu/2\,[s_{ij}-(k+1)d_{ij}]$$

$$D=\mu/2\,[s_{ij}+(k-1)d_{ij}]$$

$$E=\mu^2 r_{ij}/2$$

$$F=B+E$$

$$G=-B+E$$

The terms c_{ij}, d_{ij}, s_{ij}, and r_{ij} were defined in Eqs. (B3).

Appendix D: Vibratory Hub Loads

Flapwise, chordwise, and torsional root end blade loads can be obtained by summing the individual contributions due to the various modes. The general form is:

$$\text{Root load}=\sum_i(\text{Modal coeff.})_i(\text{Gen. coord})_i$$

where the sum includes rigid-body as well as elastic modes. The modal coefficients are summarized in Table 1. They are customary outputs in most blade natural frequency computer programs.

Expressions for the root radial loads, which are more complicated functions of the flap and chord generalized coordinates, will now be derived. Coordinate definitions are shown in Fig. 9. Material points on the blade are identified by the spanwise coordinate s. The spacial radial coordinate x, which rotates at Ω with the blade, is equal to

$$x(s)=\int_0^s\left\{1-\left(\frac{dy}{dr}\right)^2-\left(\frac{dw}{dr}\right)^2\right\}^{1/2}dr$$

$$x(s)\approx s-\tfrac{1}{2}\int_0^s\left\{\left(\frac{dy}{dr}\right)^2+\left(\frac{dw}{dr}\right)^2\right\}dr \qquad \text{(D1a)}$$

Table 1 Modal coefficients for blade root end loads

Load	Modal coefficient		
	Flap	Chord	Torsion
Shear	$\omega_{\beta i}^2\int Z_i\,dm$	$(\omega_{ci}^2+\Omega^2)\int Y_i\,dm$	...
Moment	$(\omega_{\beta i}^2-\Omega^2)\int rZ_i\,dm$	$\omega_{ci}^2\int rY_i\,dm$	$(\omega_{\theta i}^2-\Omega^2)\int I_\theta\theta_i^2\,dr$

Where it has been assumed that the blade is inextensible. The time derivatives of x are given by

$$\dot{x}(s)\approx-\int_0^s\left\{\left(\frac{dy}{dr}\right)\left(\frac{d\dot{y}}{dr}\right)+\left(\frac{dw}{dr}\right)\left(\frac{d\dot{w}}{dr}\right)\right\}dr \qquad \text{(D1b)}$$

$$\ddot{x}(s)\approx-\int_0^s\left\{\left(\frac{d\dot{y}}{dr}\right)^2+\left(\frac{d\dot{w}}{dr}\right)^2+\left(\frac{d\ddot{y}}{dr}\right)\left(\frac{dy}{dr}\right)+\left(\frac{dw}{dr}\right)\left(\frac{d\ddot{w}}{dr}\right)\right\}dr \qquad \text{(D1c)}$$

The radial and chordwise accelerations are readily found to be

$$a_X=\ddot{x}-\Omega^2x-2\Omega\dot{y} \qquad \text{(D2a)}$$

$$a_Y=2\Omega\dot{x}+\ddot{y}-\Omega^2 \qquad \text{(D2b)}$$

Equations (D1) can be substituted into (D2) to explicitly define a_X and a_Y in terms of the deflections y and w (and their derivatives). Furthermore, y and w can be expressed in terms of their modal response. That is,

$$y=\sum_i Y_i(s)v_i(t) \qquad \text{(D3a)}$$

$$w=\sum_i Z_i(s)q_i(t) \qquad \text{(D3b)}$$

Thus, the blade radial acceleration a_x can be written explicitly in terms of the generalized coordinates v_i and q_i which are readily determined from the test data. The blade root radial

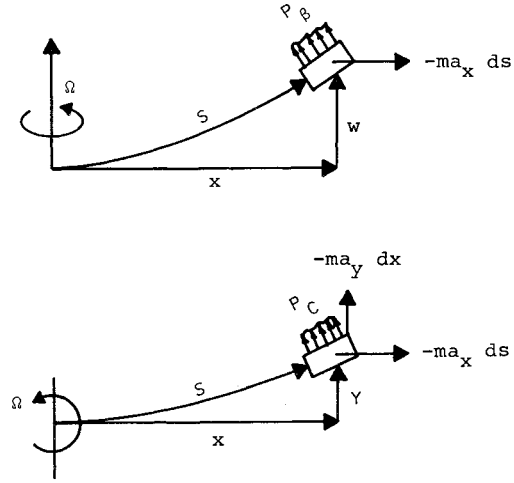

Fig. 9 Coordinate definitions.

force F_R is given by (see Fig. 9)

$$F_R = -\int_0^R \left\{ma_X + p_\beta\left(\frac{dw}{ds}\right) + p_c\left(\frac{dy}{ds}\right)\right\}ds \qquad \text{(D4)}$$

It should be noted that only aerodynamic forces make up the p's because these are "follower" forces, while Coriolus acceleration loads are not. For these circumstances, it can be shown that

$$p_\beta = \sum_j mZ_j(\ddot{q}_i + \omega_{\beta j}^2 q_j) \qquad \text{(D5a)}$$

$$p_c = 2\Omega m\dot{x} + \sum_j mY_j(\ddot{v}_j + \omega_{cj}^2 v_j) \qquad \text{(D5b)}$$

where $\dot{x}$ in Eq. (D5b) can be written in terms of v_i and q_i by using Eqs. (D1b), (D3a), and (D3b). Equations (D1) through (D5a) now allow us to evaluate F_R as a function of the generalized coordinates.

It should be realized that the steady as well as the harmonic components of the generalized coordinates contribute to the radial vibratory loads. Because it is usually difficult to accurately measure the steady bending moments, in most cases it will be necessary to calculate the steady components of the generalized coordinates theoretically. This of course makes the modal method less appealing for the determination of radial hub loads than for the determination of blade root loads in the flap and chord directions.

Acknowledgment

The encouragement and suggestions of R. Harris during the early stages of this work are appreciated.

References

[1] Ormiston, R., "Helicopter Modelling," *Aeronautical Journal*, Royal Aeronautical Society, Vol. 77, Nov. 1973, pp. 579-591.

[2] Bain, L. J., "Comparison of Theoretical and Experimental Model Rotor Blade Vibratory Shear Forces," U.S. Army Aviation Laboratories Technical Rept. 66-77, Oct. 1967.